

Final report on NCC2-5150

1.002  
IN-05-CR  
OUT

**ENHANCED MULTIOBJECTIVE OPTIMIZATION TECHNIQUE FOR  
COMPREHENSIVE AEROSPACE DESIGN**

094586

by

Aditi Chattopadhyay

Department of Mechanical and Aerospace Engineering

and

John N. Rajadas

Department of Manufacturing and Aeronautical Engineering Technology

Arizona State University

Tempe, Arizona

Technical Monitors: Dr. Eugene Tu and Dr. Scott Lawrence  
NASA Ames Research Center, Moffett Field, CA

**AN INTERCHANGE FOR JOINT RESEARCH ENTITLED**  
**ENHANCED MULTIOBJECTIVE OPTIMIZATION TECHNIQUE FOR**  
**COMPREHENSIVE AEROSPACE DESIGN**

**ABSTRACT**

A multidisciplinary design optimization procedure which couples formal multiobjectives based techniques and complex analysis procedures (such as computational fluid dynamics (CFD) codes) developed. The procedure has been demonstrated on a specific high speed flow application involving aerodynamics and acoustics (sonic boom minimization). In order to account for multiple design objectives arising from complex performance requirements, multiobjective formulation techniques are used to formulate the optimization problem. Techniques to enhance the existing Kreisselmeier-Steinhauser (K-S) function multiobjective formulation approach have been developed. The K-S function procedure used in the proposed work transforms a constrained multiple objective functions problem into an unconstrained problem which then is solved using the Broyden-Fletcher-Goldfarb-Shanno (BFGS) algorithm. Weight factors are introduced during the transformation process to each objective function. This enhanced procedure will provide the designer the capability to emphasize specific design objectives during the optimization process. The demonstration of the procedure utilizes a computational Fluid dynamics (CFD) code which solves the three-dimensional parabolized Navier-Stokes (PNS) equations for the flow field along with an appropriate sonic boom evaluation procedure thus introducing both aerodynamic performance as well as sonic boom as the design objectives to be optimized simultaneously. Sensitivity analysis is performed using a discrete differentiation approach. An approximation technique has been used within the optimizer to improve the overall computational efficiency of the procedure in order to make it suitable for design applications in an industrial setting.

## **RESEARCH STATEMENT**

### **BACKGROUND**

Design of modern day aircraft is a multidisciplinary process involving the integration of several disciplines such as aerodynamics, structures, dynamics, and propulsion. Design requirements such as aerodynamic performance, structural integrity, range, economic viability, environmental impact etc. impose wide ranging requirements on the design parameters such as the geometric shape, size, material etc. In such a complex process, optimization techniques are valuable tools that enable the designer to choose a design point for the given aircraft configuration. These optimization techniques should be able to take into account the different disciplines associated with the aircraft design simultaneously. Also, in such a multidisciplinary process, the existence of multiple design objectives and/or constraints is inevitable. This requires that the optimization technique be capable of addressing multiple design objectives and constraints. This can be a difficult task because desired performance criteria in the different disciplines involved in the design process often lead to conflicting requirements on vehicle configurations. Since such an optimization problem involves the coupling of many design objectives, the objective function formulation is complicated. A common approach for addressing such a design problem is to combine the various objective functions linearly using weight factors. Such a procedure does not satisfy the necessary Kuhn-Tucker conditions of optimality. Also, the proper choice of the weight factors, which is based primarily on the designer's intuition and experience, is critical in such a design process. A more rigorous approach is therefore required in establishing appropriate mathematical formulations for such a problem. There are a number of optimization procedures that are capable of addressing this aspect [1]. One such optimization technique is the Kreisselmeier-Steinhauser (K-S) function approach [2,3]. The K-S technique is a multiobjective optimization technique that combines all the objective functions and the constraints to form a single unconstrained composite function to be minimized. An appropriate unconstrained solver is then used to locate the minimum of the composite function. Any application where there is more than one design criteria to optimize is a candidate for this method. The K-S technique has already been shown to be effective in various applications such as Tilt-Rotor design, High-Speed Civil Transport(HSCT) design, wing design, sonic boom minimization in HSCT, etc. [4-6]. This approach, which is not judgmental in nature, enables the designer to avoid using weight factors in the optimization problem formulation. However, the aircraft design process being inherently hierarchical in nature, certain design criteria may often require more emphasis than others. For example, in the design of high speed aircraft, sonic boom minimization may require a larger emphasis than improvements in the lifting characteristics of the wing which already is at a near

optimal design configuration. In the present work, a technique has been formulated to allow the designer to have this capability, while preserving the original unweighted, user input-free optimization capability. Thus, the new method is more versatile and lends itself to application in both preliminary as well as detailed designs. The approach has been to modify the K-S functions using weight factors (unlike the usual way of equal weights on all the objective functions), thus enabling increased emphasis on specific objectives during the optimization process. This has been achieved by multiplying the normalized objective functions of the original K-S function technique with weight factors. The resultant new technique is heretofore referred to as the enhanced K-S function technique.

The enhanced K-S multiobjective formulation technique has been applied to a number of optimization problems with varying degrees of complexity which include both a classical three bar truss problem and a HSCT sonic boom minimization problem. Both of these problems exhibit conflicting design requirements. The three bar truss problem has been chosen to demonstrate the effectiveness of the method by comparing it to a known optimization problem. The use of the technique on the HSCT problem shows the effectiveness of the enhanced K-S method on a modern day aerospace application. The HSCT problem has competing design criteria that must be optimized. For example, minimum drag-to-lift ratio ( $C_D/C_L$ ) requires a slender forebody whereas minimum sonic boom designs usually have blunt forebodies. The following sections briefly outline the enhanced K-S function approach and the two problems used to demonstrate the procedure. More detailed information about the problems and the K-S approach can be found in the cited references and the following sections.

## **OBJECTIVES**

The objectives of the present research effort were as follows.

- (a) Refine the enhanced K-S function approach for multiobjective formulation by examining the aspect of scaling the weight factors in order to achieve consistent optimum designs.
- (b) Demonstrate the enhanced multiobjective design optimization procedure by addressing the problem of minimizing sonic boom while improving aerodynamic performance characteristics of high speed transport aircraft configurations using a variety of objective function combinations.

## **APPROACH**

The overall approach has been to enhance the K-S function formulation, which is capable of addressing multiple design objectives simultaneously, by adding weight factors to each objective function. This formulation has been coupled to a comprehensive, three dimensional CFD solver [7] to evaluate the flow field of the aircraft configuration being optimized. Appropriate sensitivity analysis been used during optimization. Efforts have been taken to ensure computational efficiency of the overall procedure. Relevant details of the analysis and optimization procedures along with the outline of the enhancement technique are described in the following sections. Representative results obtained by the preliminary application of the enhancement procedure are also given.

### **Multiobjective Formulation**

The design process associated with modern aircraft development is complex. Multiple design criteria with varying degrees of importance must be addressed. Very restrictive constraints are usually imposed in order to make the overall design a viable one from the user's perspective. Therefore careful attention must be given to the selection of the techniques used in the optimization procedure so that the resultant procedure is efficient, accurate, robust and easily adaptable to changing design requirements.

#### **A multiobjective optimization problem:**

An optimization problem with multiple design objectives can be stated as follows.

$$\begin{aligned}
 &\text{Minimize or maximize} \quad F_k(\phi_n), \quad k = 1, 2, \dots, \text{NOBJ} \quad (\text{objective functions}) \\
 &\quad \quad \quad n = 1, 2, \dots, \text{NDV} \\
 &\text{subject to} \\
 &\quad \quad \quad g_j(\phi_n) \leq 0 \quad j = 1, 2, \dots, \text{NCON} \quad (\text{inequality constraints}) \\
 &\quad \quad \quad \phi_{nL} \leq \phi_n \leq \phi_{nU} \quad (\text{side constraints})
 \end{aligned}$$

where NOBJ denotes the number of objective functions, NDV is the number of design variables and NCON is the total number of constraints. The subscripts L and U represent lower and upper bounds, respectively, on the design variable  $\phi$ .

A variety of multiobjective techniques are available today and it is important to evaluate the best formulation procedure appropriate for a given application. Based on the experience gained on using a variety of multiobjective techniques on a wide spectrum of applications, the K-S function approach [2,3] has been chosen for the proposed work. This technique (before enhancement) has been successfully demonstrated on related applications by the Principal Investigators (PIs) [1,4-6]. Brief description of the method is given below.

Kreisselmeier-Steinhauser (K-S) function approach:

In the K-S function approach, the original objective functions are transformed into reduced or normalized objective functions [3]. Depending on whether these functions are to be minimized or maximized (Eqns. 1a or 1b), they can be expressed as,

$$\hat{f}_i(\Phi) = \frac{F_i(\Phi)}{F_{i_0}} - 1.0 - g_{\max} \leq 0 \quad i = 1, \dots, NF \quad (1a)$$

$$\hat{f}_i(\Phi) = 1.0 - \frac{F_i(\Phi)}{F_{i_0}} - g_{\max} \leq 0 \quad i = 1, \dots, NF \quad (1b)$$

where  $F_{i_0}$  represents the value of the original objective function at the current reference design variable vector for a given iteration, and  $F_i$  is the value of the original objective function which is dependent on the design variable vector.  $F_{i_0}$  is constant for a whole iteration. The quantity  $g_{\max}$  is the largest value of the original constraint vector at the current reference point and is held constant during each iteration. Since the reduced objective functions are analogous to the original constraints, a new constraint vector  $f_m(\Phi)$ ,  $m = 1, 2, \dots, M$  where  $M = NC + NF$ , is introduced. The first  $NC$  elements of  $f_m$  are the original constraints of the problem and the next  $NF$  elements are the reduced objective functions. The original constrained optimization problem with multiple objective functions is thus transformed into a single-objective, unconstrained minimization problem using the K-S function, as

Minimize

$$F_{KS}(\Phi)$$

where

$$F_{KS}(\Phi) = f_{\max} + \frac{1}{\rho} \log_e \sum_{m=1}^M e^{\rho(f_m(\Phi) - f_{\max})} \quad (2)$$

where  $f_{\max}$  is the largest constraint corresponding to the new constraint vector  $f_m(\Phi)$  (in general not equal to  $g_{\max}$ ). When the original constraints are satisfied during optimization, the constraints due to the reduced objective functions are violated. Initially, in an infeasible design space, where the original constraints are violated, the constraints due to the reduced objective functions are satisfied (i.e.,  $g_{\max}$  is negative). The optimizer attempts to satisfy the violated constraints, thus optimizing the original objective functions ( $F_i$ ). The multiplier  $\rho$ , which is analogous to the draw-down factor of penalty function formulation, controls the distance from the surface of the K-S envelope to the surface of the maximum constraint function. When  $\rho$  is large, the K-S function will closely follow the surface of the largest constraint function and when  $\rho$  is small, the K-S function will include contributions from all constraints. The new unconstrained minimization problem can be solved by using a variety of techniques. In the present work, the Broyden-Fletcher-Goldfarb-Shanno (BFGS) algorithm [8] has been used. This algorithm approximates the inverse of the Hessian of the composite objective function using a rank-two update and guarantees both symmetry and positive definiteness of the updated inverse Hessian matrix.

An example of the application of the K-S function formulation is illustrated in Figs. 1-2 for an optimization problem with two objective functions to be minimized and one constraint. The objective functions and the constraint are functions of a single design variable,  $\phi$ . An initial design point of  $\phi_0 = 0.5$  is used in the example. At this point, the constraint is satisfied and, therefore,  $g_{\max}$  is negative. The original constraint and the two additional constraints from the two reduced objective functions, calculated from Eq. 1a, are shown in Fig. 2 along with the K-S function envelopes for two different values of  $\rho$ . Since  $g_{\max}$  is negative, the constraints due to the two reduced objective functions are positive and hence, violated, at the initial design point,  $\phi_0$ . It is seen in Fig. 2 that for  $\rho = 1$ , the K-S function includes contributions from all the three constraints. For the larger value of  $\rho = 3$ , the K-S function gets a stronger contribution from the largest constraint and weaker contributions from the other two. Thus large values of  $\rho$  “draw down” the K-S function closer to the value of the largest constraint. The value of  $\rho$  may change from cycle to cycle in the optimization process. It is progressively increased so that, as the optimization

proceeds, the K-S function more closely represents only the largest constraint (or the most violated reduced objective function).

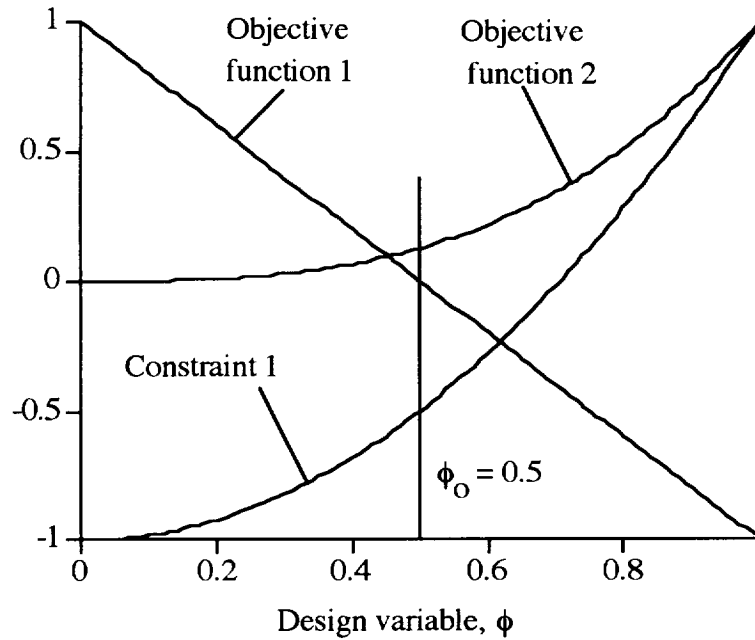


Figure 1. Original objective functions and constraints.

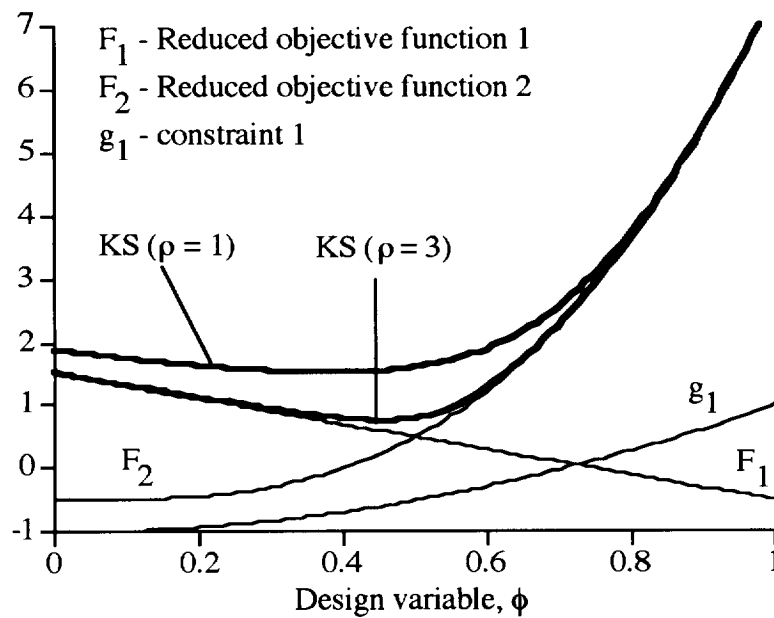


Figure 2. K-S function envelope.



### Enhanced K-S Function Technique

As mentioned above, the main focus of the present work is to enhance the K-S approach described in the previous section which will enable the user to emphasize specific objective functions. Towards this end, the reduced objective functions have been modified to allow relative weighting of specific design criteria. This is achieved by incorporating a vector of weight factors  $\beta_i$  ( $i = 1, 2, \dots, NF$ ) in the K-S envelope as shown below.

$$\hat{f}_i(\Phi) = \frac{\beta_i F_i(\Phi)}{F_{i_0}} - \beta_i - g_{\max} \quad i = 1, \dots, NF \quad (3)$$

The total number of weight factors is equal to the number of objective functions. The relative magnitudes of  $\beta_i$  will help to emphasize specific objective functions in the overall optimization process. The weight factors ( $\beta_i$ ) are positive numbers the numerical values of which are dictated by the specific application. The original unweighted K-S formulation is recovered if  $\beta_i = 1$ .

In the present work, two different methods of weighting were investigated. The first one involved assigning positive integer values larger than unity as the weight factor for the objective function to be emphasized, while assigning a weight factor of unity to all other objective functions. The second assigned unity to be the weight factor for the emphasized objective function, while assigning a positive value smaller than unity to the remaining objective functions. In the sections below, the following definitions are employed to identify the two methods described above.

**Type A :** Weight factors for emphasized objective functions are positive integer value larger than unity, while all other weight factors are assigned a value of unity.

**Type B :** Weight factor for emphasized objective function is unity, while all other weight factors take on values less than unity.

### Sensitivity Analysis

Sensitivity analysis is an essential part of any gradient-based design optimization procedure. Since a CFD-based, 3D Navier Stokes solver is used for aerodynamic analysis, the use of standard finite difference techniques for calculation of the design sensitivities can be computationally prohibitive. Therefore, a discrete semi-analytical sensitivity analysis procedure developed by Chattopadhyay and Pagaldipti [9] will be used to calculate the aerodynamic design sensitivities including the sonic boom sensitivities.

### Approximate Analysis

The optimization technique used in this research is gradient-based and requires the evaluation of the objective functions and constraints during every iteration of optimization. For the HSCT problem, it is computationally expensive to evaluate these functions through exact analysis all the time. Here, an approximate analysis technique has been used within each iteration of the optimization. The two-point exponential approximation technique developed by Fadel et al. [10], has been found to be well suited for nonlinear optimization problems and has been used in the present research for approximating the objective functions and the constraints within each optimization cycle. The technique is formulated as follows.

$$\hat{F}(\Phi) = F(\Phi_1) + \sum_{n=1}^{NDV} \left[ \left( \frac{\phi_n}{\phi_{1n}} \right)^{p_n} - 1.0 \right] \frac{\phi_{1n}}{p_n} \frac{\partial F}{\partial \phi_n}(\Phi_1) \quad (4)$$

where  $F_i(\Phi)$  is the approximation to the objective function  $F_i$  at a neighboring design point  $\Phi$ , based on its values and its gradients at the current design point  $\Phi_1$  and the previous design point  $\Phi_0$ . The approximate values for the constraints,  $g_j(\Phi)$ , are calculated in a similar fashion. This technique takes its name from the fact that the exponent used in the expansion is based upon gradient information from the previous and current design cycles. The exponent  $p_n$ , in Eq. 4 is defined as:

$$p_n = \frac{\log_e \left\{ \frac{\partial F}{\partial \phi_n}(\Phi_0) \right\} - \log_e \left\{ \frac{\partial F}{\partial \phi_n}(\Phi_1) \right\}}{\log_e \left\{ \phi_{0n} \right\} - \log_e \left\{ \phi_{1n} \right\}} + 1.0 \quad (5)$$

$p_n$  can be considered as a “goodness of fit” parameter, which explicitly determines the trade-offs between traditional and reciprocal Taylor series based expansions (also known as a hybrid approximation technique). It can be seen from Eq. 4 that, in the limiting case of  $p_n = 1$ , the expansion is identical to the first order Taylor series and when  $p_n = -1$ , the two-point exponential approximation reduces to the reciprocal expansion form. In the present work, the exponent is defined to lie within this interval ( $-1 \leq p_n \leq 1$ ). Equations 4 and 5 indicate that singularity points may exist in the use of this method and care must be taken to avoid such points. In the present study, when singularity problems arise, the approximation technique is reduced to the linear Taylor series expansion ( $p_n = 1$ ).

In multidisciplinary optimization, competing design attributes are almost always present. The following problems all have the property of having objective functions that impose conflicting design requirements. Three different problems have been chosen to demonstrate the enhanced K-S formulation. The first is an algebraic example problem with two objective functions, two constraints, and one design variable. The second is a classical three bar truss problem with two objective functions, six structural constraints, and two design variables [3]. The last problem is associated with HSCT that has three objective functions, three constraints, and six design variables.

## RESULTS & DISCUSSION

### a) 3-Bar Truss Problem

The first application of the enhanced K-S function is a classical three bar truss problem [3]. The problem addressed here is a modified version of the one that the original K-S formulation was demonstrated on in Ref. 3. A schematic of the problem is shown in Figure 3. The two outside bars of the truss are made of steel, and the middle bar is made of titanium. Two loads are applied as shown. The material properties and costs of the bars are also shown on the figure. The design objectives are to minimize both the weight and cost of the truss. The formulation of the problem is as follows.

Minimize

Weight of the 3-Bar truss,  $W$

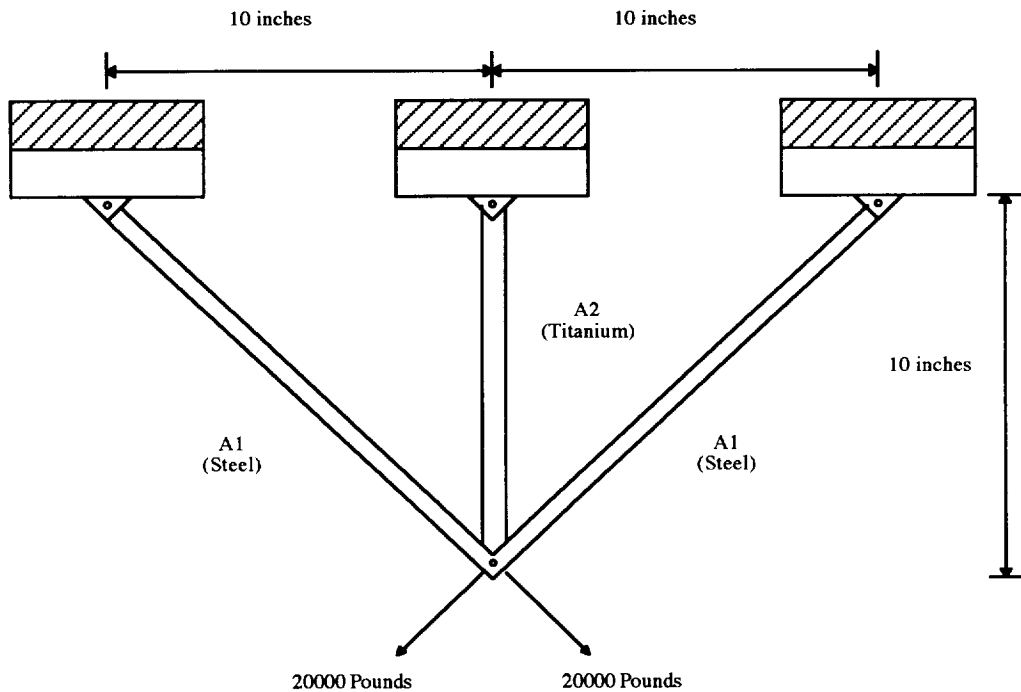
Cost of the 3-Bar truss,  $C$

subject to

$$S_a \leq S_i \leq S_{yt} \quad i = 1 - 3$$

The aim is to minimize the weight of the truss while minimizing its cost. There are two objective functions, six constraints, and two design variables in the optimization problem. The design variables are the cross sectional areas of the truss members,  $A_1$  and  $A_2$ , (Figure 3) which are required to be greater than 0.001 square inches. There are three constraints on the tensile loads and three on the compressive loads. Since titanium is lighter than steel the minimum weight design would use a larger titanium center member and smaller steel outer members. Since steel is cheaper than titanium, the minimum cost design would have a smaller titanium center member and larger

steel outer members. These conflicting design criteria make this problem a good candidate for demonstrating the enhanced K-S technique.



Material Properties	Steel	Titanium
Young's Modulus(psi)	30,000,000	15,500,000
Density (lb/cu in)	0.282	0.160
Cost(\$/lb)	0.41	25.00
Tensile Yield Stress(psi)	36,000	110,000
Comp. Yield Stress(psi)	27,000	82,500

Figure 3. Three Bar Truss Example Problem with Material Properties.

Preliminary optimization was carried out for the three reference cases (see Figs. 4-5):

- (i) Single objective, weight minimization ("weight only")
- (ii) Single objective, cost minimization ("cost only") and
- (iii) Multiobjective, unweighted optimization ("(1,1)").

These are used as references for the enhanced optimization. The expected trends of weight and cost variations are seen. Also, Figure 5 indicates that the minimum cost criteria is the critical one in this optimization problem. The results obtained by using the enhanced multiobjective optimization process on the 3-Bar Truss Problem are presented in Figures 6-9. In the figures, the weight factor set (5,1) means that the first objective function (weight) has received a weight factor of 5 while the second (cost) has a weight of 1. The unweighted K-S formulation is recovered when a combination of (1,1) is applied.

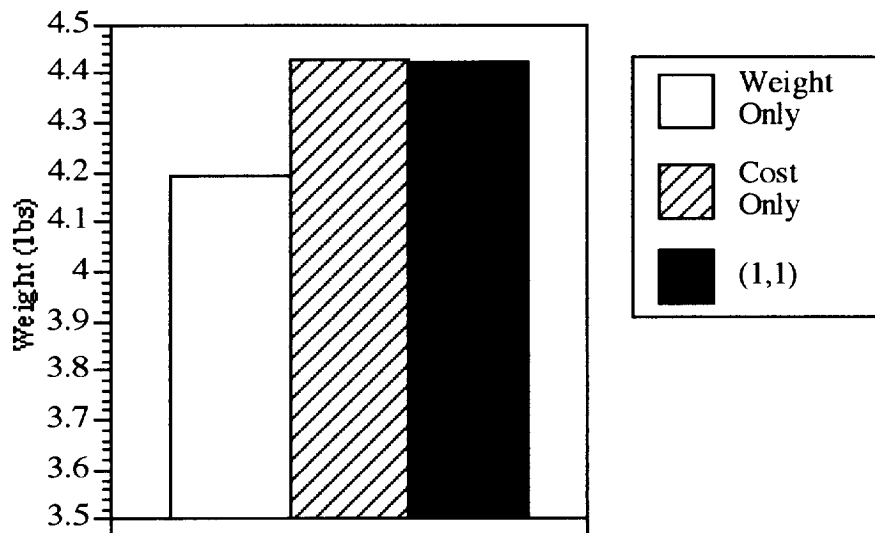


Figure 4. 3-Bar Truss: Weight.

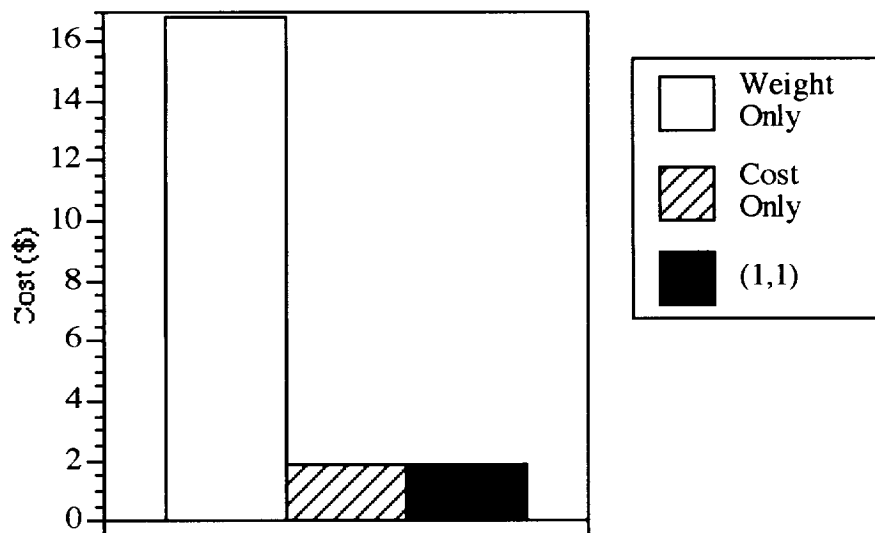


Figure 5. 3-Bar Truss : Cost.

Figures 6-7 show the results of weighting the first objective function (weight) using Type A weight factors. Weight factors of 2, 5, 10, and 100 relative to the cost have been chosen to emphasize the minimum weight criterion here. The results show that the enhanced K-S approach is effective in emphasizing a specific objective in the multiobjective optimization problem. For example, when weight of the truss is emphasized (Fig. 6), the decrease in weight with increasing emphasis (weight factor varies from 1 to 10) is seen.

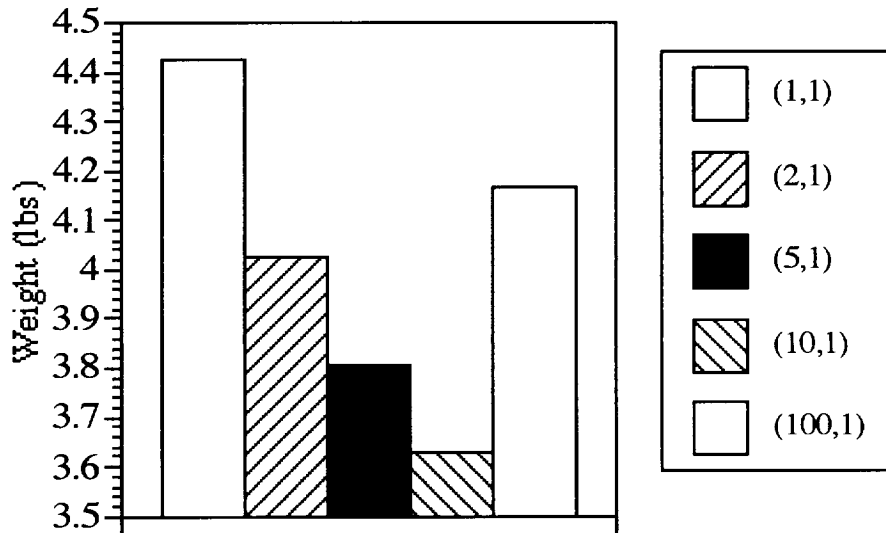


Figure 6. Weight for Type A Weight Factors.

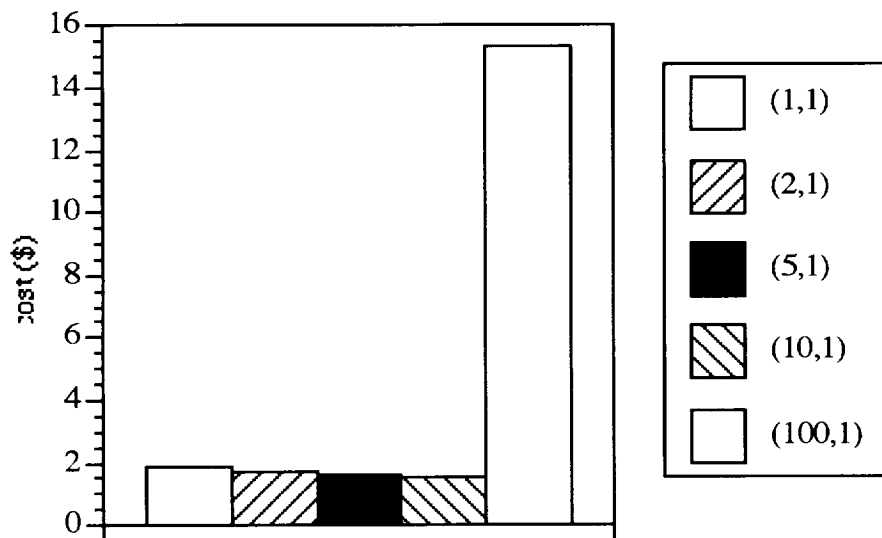


Figure 7. Cost for Type A Weight Factors.

The effect of the weighting on the design variables is shown in Table 1, which also contains the tensile force constraint for the steel bars that was violated consistently.

Table 1. Effect of Weight Factors on Design Variables and Violated Constraint.

Weight Factor Sets	A1 (in <sup>2</sup> )	A2 (in <sup>2</sup> )	Violated Constraint
(1,1)	0.555	0.001	0.00085
(2,1)	0.505	0.001	0.09974
(5,1)	0.477	0.001	0.16423
(10,1)	0.455	0.001	0.22047
(100,1)	0.442	0.318	0.00636
(1,0.5)	0.555	0.001	0.00050
(1,0.2)	0.555	0.001	0.00022
(1,0.1)	0.555	0.001	0.00013
(1,0.01)	0.453	0.347	0.00011

Figures 8-9 show the results of the Type B weight factors de-emphasizing the cost, thus emphasizing the weight. From the table and the figures, it is apparent that the Type B weight factors did have the expected effect, however it took a fairly small weight factor to eventually achieve it. In the intermediate range, the de-emphasizing of the Cost objective function actually allowed the constraint that was being violated to get smaller and smaller. Finally, at (1,0.01), the objective function for weight was emphasized sufficiently to cause it to decrease significantly, simultaneously causing the cost to increase substantially.

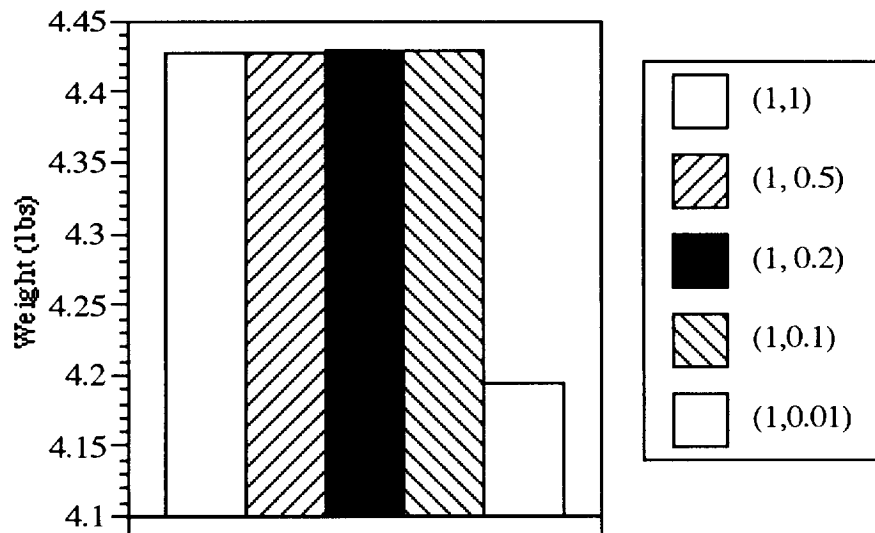


Figure 8. Weight for Type B Weight Factors.

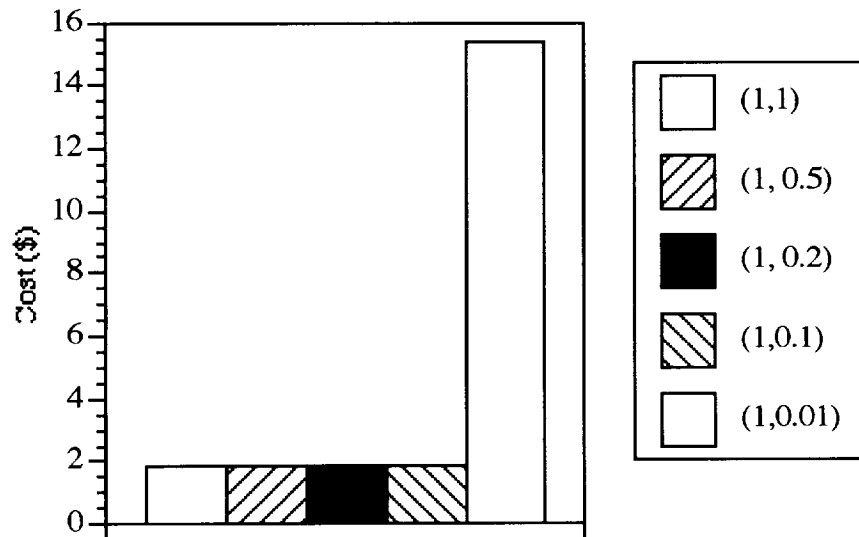


Figure 9. Cost for Type B Weight Factors.

As mentioned above, the numerical values of the weight factor(s) depend on the application at hand. User input and competence thus are important factors in the optimization process. The change in the objective function with increasing weight factor is nonlinear. That is, a very large value of the weight factor does not always lead to the lowest value of the objective function. The reason for that is, the effect of weight factors on the K-S function envelope is nonlinear and hence a particularly large weight factor may have the effect of forcing the design into the infeasible domain leading to infeasible designs. It appears that the Type B weight factors are preferable



because they can achieve the desired effect (with correct user input) while not violating the constraints to the same extent as the original K-S formulation does.

#### b) HSCT Sonic Boom Problem

The second problem addressed in this work is that of a High Speed Civil Transport design for minimum sonic boom and improved aerodynamic performance [5-7]. Figure 10 illustrates a schematic of the sonic boom pressure signature produced by a supersonic wing-body configuration at a given distance from the aircraft. The two positive pressure peaks are the sonic boom levels

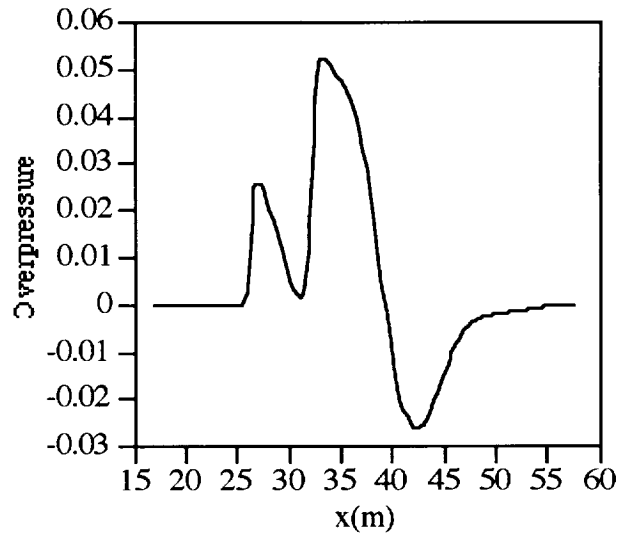


Figure 10. Sonic boom pressure signature of a supersonic aircraft configuration.

that must be minimized. The first peak is associated with the shock wave caused by the nose of the aircraft. The second peak is caused by the wing. The negative pressure peak corresponds to the expansion waves that occur in the flow field past the wing. From an aerodynamics perspective, it is of interest to minimize the ratio of the coefficient of drag to the coefficient of lift ( $C_D/C_L$ ). Thus, the three objective functions to be minimized for this optimization problem are the two pressure peaks and the  $C_D/C_L$  ratio. This must be accomplished while keeping the lift at a desired level, which is done by imposing upper and lower limits on the  $C_L$  ( $C_{L_{max}}$  &  $C_{L_{min}}$ ). A constraint has also been placed on the wing trailing edge angle to ensure computational stability. There are also upper and lower limits (constraints) imposed on the design variables. The mathematical formulation of the problem is as follows.

Minimize

Drag to Lift Ratio,  $C_D/C_L(1)$

Overpressure Peaks,  $\Delta p_{\max_1}(2), \Delta p_{\max_2}(3)$

subject to

$$C_{L_{\min}} \leq C_L \leq C_{L_{\max}}$$

Lift Constraint

$$\lambda_{te} \leq \frac{\pi}{2} \text{ rad}$$

Wing Trailing Edge Constraint

$$\Phi_L \leq \Phi \leq \Phi_U$$

Side Constraints on Design Variables

In the present work, since all the design variables that were chosen are associated with the wing geometry, they only have significant effects on the second pressure peak and the  $C_D/C_L$  ratios. So, these will be the objective functions that are addressed here. The nose length and the maximum radius of the forebody are held constant at a level commensurate with (obtained separately) minimum first pressure peak during the optimization of  $\Delta p_{\max_2}$  and  $C_D/C_L$ .

The design variables for this configuration are shown on Figure 11. The six design variables are wing root chord ( $c_O$ ), the two leading edge sweeps ( $\lambda_1$  &  $\lambda_2$ ), tip chord ( $c_I$ ), break length ( $x_b$ ), and wing starting location ( $x_W$ ). As mentioned previously, upper and lower bounds are imposed on these variables during the optimization process. While the first pressure peak remains an objective function, only the second pressure peak and the  $C_D/C_L$  ratio will be weighted since the variables that affect the first pressure peak are not included in the design variable set.

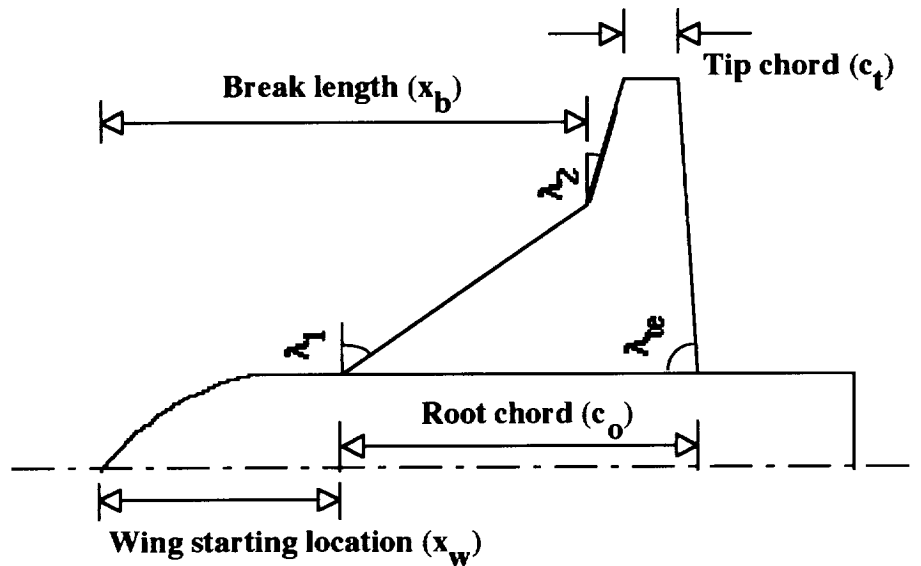


Figure 11. HSCT configuration and design variables.

### Aerodynamic Analysis

In this research, the flow field for the HSCT has been evaluated using a flow solver called UPS3D [11] that utilizes the three dimensionalized Parabolized Navier Stokes (PNS) equations. The assumptions made in deriving the PNS equations are outlined below [11-13]. The streamwise derivatives of the viscous terms are neglected. The inviscid region of the flow field must be supersonic and the streamwise velocity component must be positive everywhere. Thus streamwise flow separation is not allowed but crossflow separation is allowed. Unlike the unsteady Navier-Stokes equations which require time marching numerical schemes, the PNS equations are solved using space marching schemes resulting in significant reductions in computational time and memory requirements. The flow solver is the UPS3D code [11] developed at NASA Ames Research Center. The computational procedure used in this code integrates the PNS equations using an implicit, approximately factored, finite-volume algorithm where the crossflow inviscid fluxes are evaluated by Roe's flux-difference splitting scheme [14]. The UPS3D code also has the capability of calculating the inviscid flow field, by solving the PNS equations without the viscous terms. In the present research, this inviscid option has been used while evaluating the flow field. The upwind algorithm is used to improve the resolution of the shock waves over that obtained with the conventional central differencing schemes. The post-processor in the UPS3D solver evaluates the non-dimensional force coefficients, such as lift coefficient ( $C_L$ ) and drag coefficient ( $C_D$ ), by integrating the pressure distributions over the surface of the body. Non-dimensionalization of these force coefficients is performed using a user-specified characteristic area of the aircraft

### Sonic Boom Analysis

Cheung et al. [15] have combined Whitham's quasilinear theory [16] with the three-dimensional PNS code, UPS3D, to predict sonic boom. The flow field associated with wing-body configurations is evaluated by UPS3D and the overpressure signal for the near field is evaluated. The overpressure signals at specified far fields are then obtained using one of three different approaches for various configurations such as a cone-cylinder, a low aspect-ratio rectangular wing and a delta wing-body. In the first approach (for nonlifting cases), the UPS3D code is modified so as to incorporate a sonic boom prediction capability including all nonlinear effects. The second approach is applicable to both lifting and nonlifting cases. In this approach, an extrapolation method [17] has been used for predicting sonic boom. In the third approach (for lifting cases), the equivalent area distribution due to lift is generated by the surface pressure coefficients calculated by the CFD solver. The equivalent area distribution due to volume is calculated from the geometry of the aircraft. Summation of the two equivalent area distributions yields the total equivalent area distribution that gives the F-function of the body. In the present research, the second approach, based on the extrapolation technique of Ref. 17, has been used to obtain the sonic boom signatures.

### Sonic Boom Results

The enhanced K-S formulation has been applied to the High Speed Civil Transport configuration described above. For the weighting factors, the order of the objective functions ( $F_i$ ) is,  $C_D/C_L$  ( $i = 1$ ), then the first and second pressure peaks ( $i = 2, 3$ ). Thus, a (5,1,1) weight factor set indicates that  $C_D/C_L$  is weighted by a factor of 5 relative to  $(\Delta p_{\max})_1$  and  $(\Delta p_{\max})_2$ . The "ref" indicates the configuration before the optimization process begins. As mentioned previously, for the present work only the first and third objective functions will be assigned weighting factors. All the results were for  $d_1 = 3.61 l_b$  and were based on 30 cycles of optimization.

One key element of the optimization problem is the evaluation of design sensitivities for the HSCT application, these sensitivities were obtained using a finite difference approach where the design variables are perturbed by a prescribed amount and the CFD solver is used on the "perturbed" configurations. The results from the perturbed and unperturbed configurations are used for calculating the sensitivities. This has its inherent accuracy problems in addition to the large computational time involved. Also, the 2-point exponential approximation technique used to advance from cycle to cycle may also give rise to deviations from a true design point. Such deviations and errors may sometimes be magnified if the problem under consideration (e.g. HSCT)

is complex involving large analysis tools. The results of the present section should be viewed with these considerations as a backdrop.

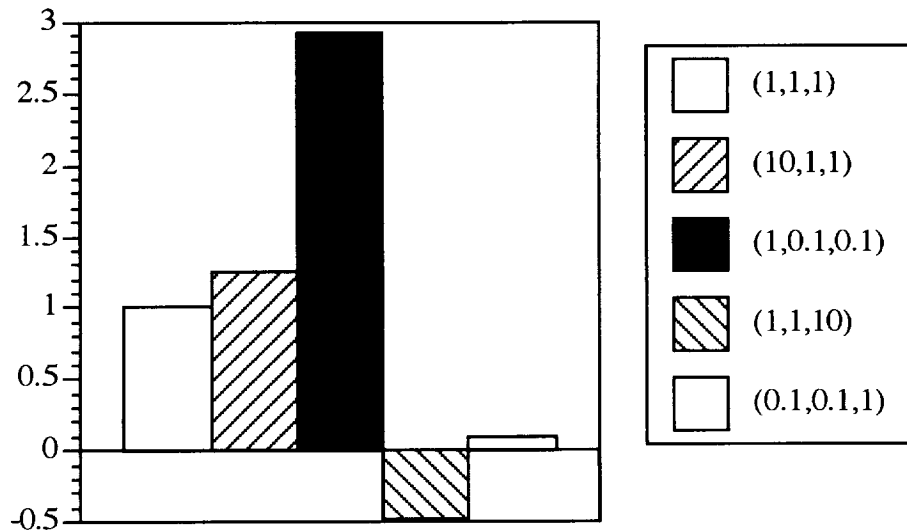


Figure 12. Theoretical Percent Reduction for  $C_D/C_L$ .

In Figures 12-13, the theoretical reductions per cycle for each objective function are illustrated in a comparative fashion. The actual values of the reductions are contained in Table 2. An examination of the figures and table show that the weight factors appear to be effective. It would be expected that when one of the objective functions is emphasized either by being directly weighted or by de-emphasizing the other functions, its percent reduction will increase. As apparent from the data, this does not always mean that the percent reduction for that function will be greater than for the unweighted case, but that it will have increased in importance relative to the other functions.

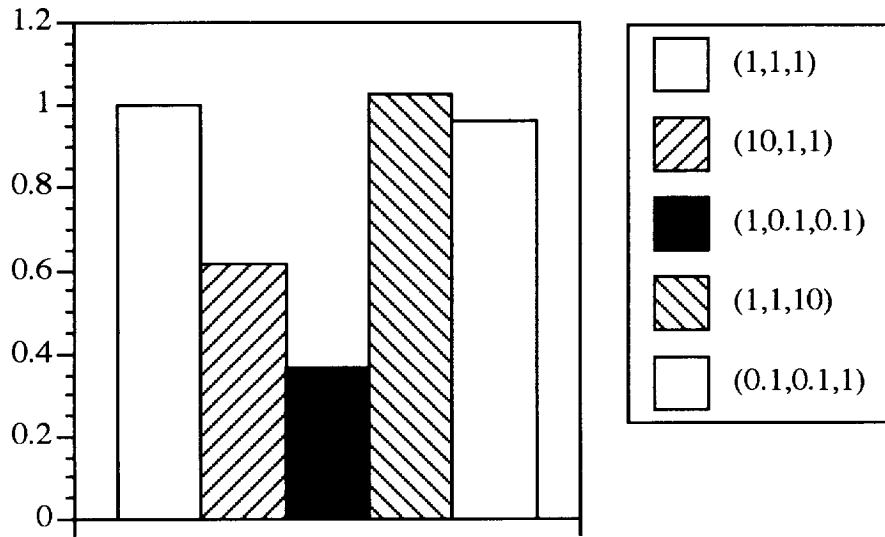
Figure 13. Theoretical Percent Reduction for  $(\Delta p_{\max})_2$ .

Table 2. Theoretical percent reductions for objective functions.

Weight Factor Sets	$C_D/C_L$	$(\Delta p_{\max})_2$
(1,1,1)	0.354	6.023
(10,1,1)	0.440	3.729
(1,0,1,0,1)	1.034	2.207
(1,1,10)	-0.168	6.193
(0,1,0,1,1)	0.033	5.820

Looking first at the percent reductions when  $C_D/C_L$  is emphasized, both Type A and B weight factors show an increase in the percent reduction of  $C_D/C_L$  and a decrease in the percent reduction of  $(\Delta p_{\max})_2$ . For the case where  $(\Delta p_{\max})_2$  is emphasized, the Type A weight factor set shows a small increase in percent reduction for  $(\Delta p_{\max})_2$  and a significant decrease in the percent reduction of  $C_D/C_L$ . In fact,  $C_D/C_L$  actually experienced a theoretical percent gain instead of reduction in each cycle on average. The Type B weight factor set does have a small decrease in the percent reduction of the emphasized function, but it also has a very significant decrease in the percent reduction for the de-emphasized function. This equates to the emphasized objective function being more sensitive to design changes than in the unweighted case.

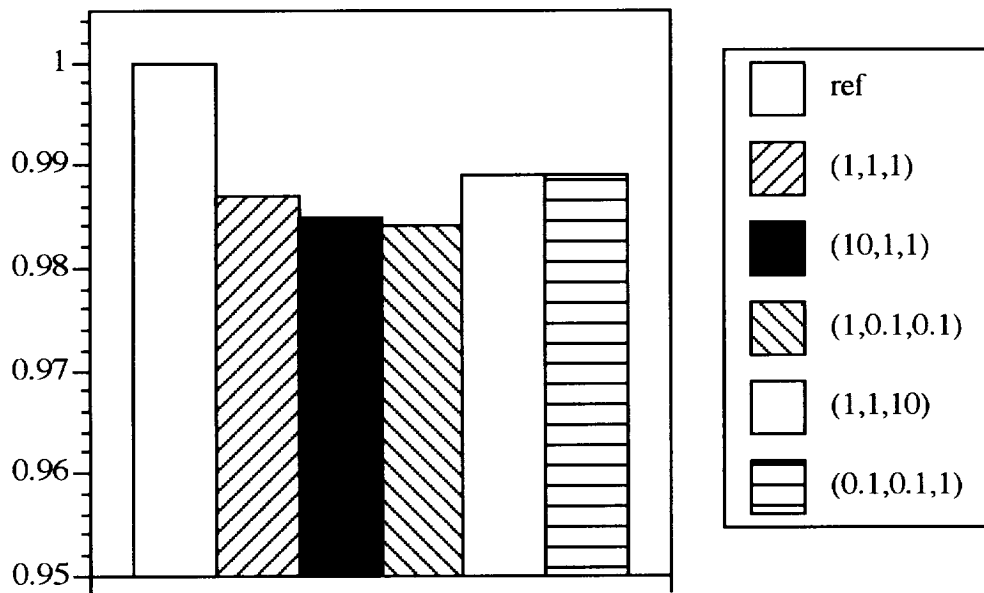


Figure 14. Comparative results of minimum  $C_D/C_L$  for each weight factor set.

Figures 14-15 show the effect of the weight factors on the objective functions. The optimum solutions (after 30 cycles) obtained for unweighted ((1,1,1)),  $C_D/C_L$ -emphasized ((10,1,1) and (1,0,1,0.1)) and  $(\Delta p_{\max})_2$ -emphasized ((1,1,10) and (0.1,0.1,1)) are compared along with the reference values of the objective functions of interest ( $C_D/C_L$  and  $(\Delta p_{\max})_2$ ). Tables 5-6 also contain the minimum values achieved for  $C_D/C_L$  and  $(\Delta p_{\max})_2$  for each weight factor set. Also shown in the tables are the corresponding design variables for these cases and at which iteration they occurred.

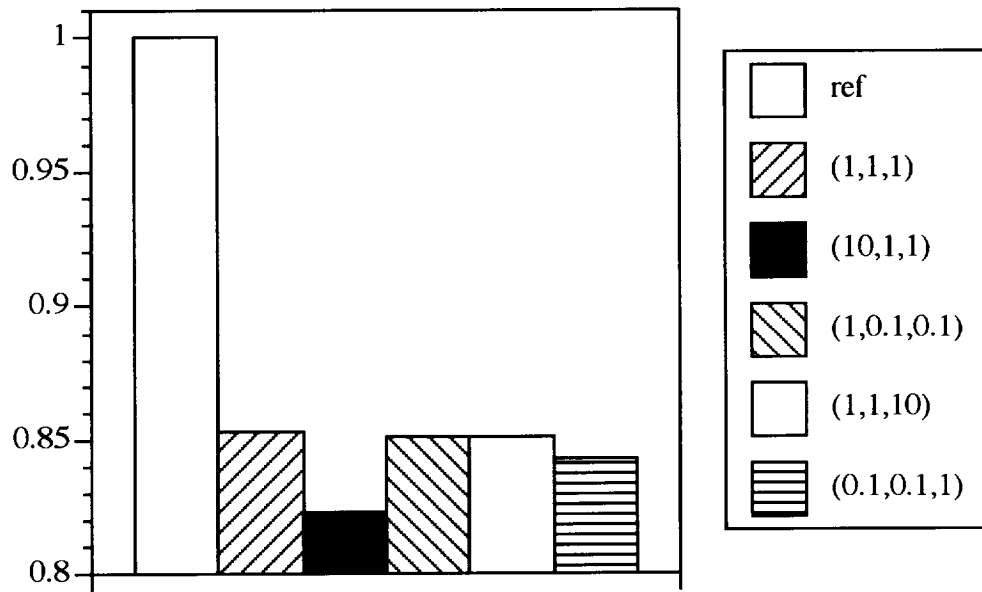


Figure 15. Comparative results of minimum  $(\Delta p_{\max})_2$  for each weight factor set.

It is apparent from Figure 14 and Table 3 that for the minimum  $C_D/C_L$  case, the results reflect what was expected. The weight factor sets that emphasized  $C_D/C_L$  achieve a lower  $C_D/C_L$  than the unweighted case, and the weight factor sets that emphasize  $(\Delta p_{\max})_2$  have a larger minimum  $C_D/C_L$  than the unweighted case. For the minimum  $(\Delta p_{\max})_2$  cases, there is a little explanation required for the results. Figure 15 and Table 4 show that all the weight factor sets achieved lower values for  $(\Delta p_{\max})_2$  than the unweighted case. The lowest minimum was found with the Type A weight factor set even though it is designed to emphasize  $C_D/C_L$ . It must be noted that this set did in fact achieve the results desired for emphasizing  $C_D/C_L$ . The main reason for the occurrence of the lower value of  $(\Delta p_{\max})_2$  here could be that the optimization formulation tends to favor the objective function with the lowest value  $((\Delta p_{\max})_2)$ , as explained earlier. This can be seen from Tables 3-4, where even though  $C_D/C_L$  definitely grows in importance when weighted for the cases chosen,  $(\Delta p_{\max})_2$  still has a larger theoretical percent reduction. Also, the approximation procedure (two-point exponential) used within each optimization cycle contributes to slight deviations in the solutions, especially at intermediate cycles.



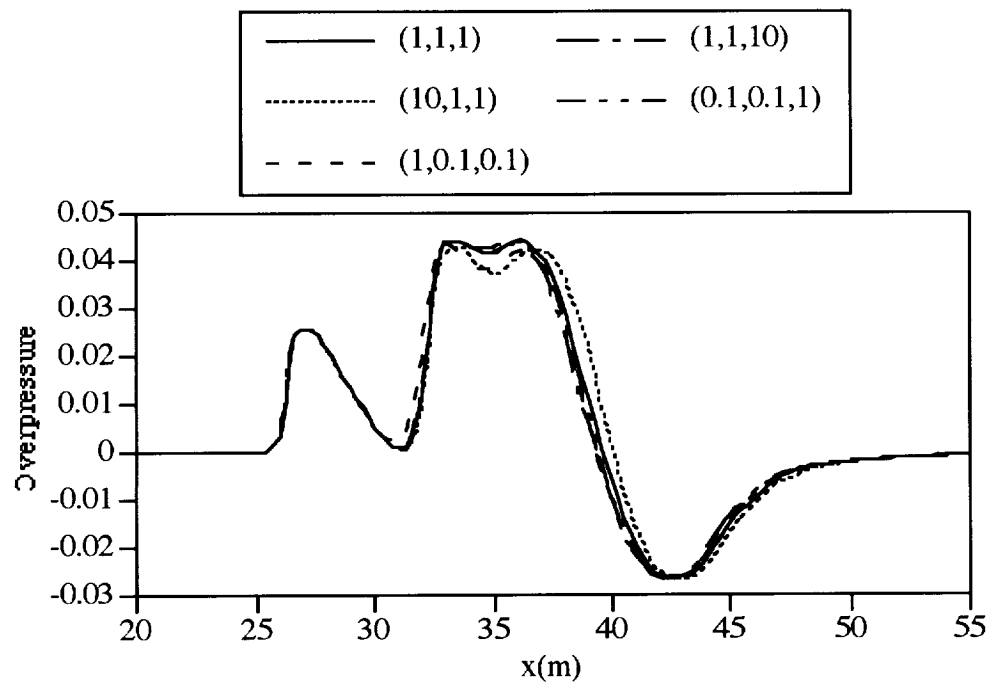
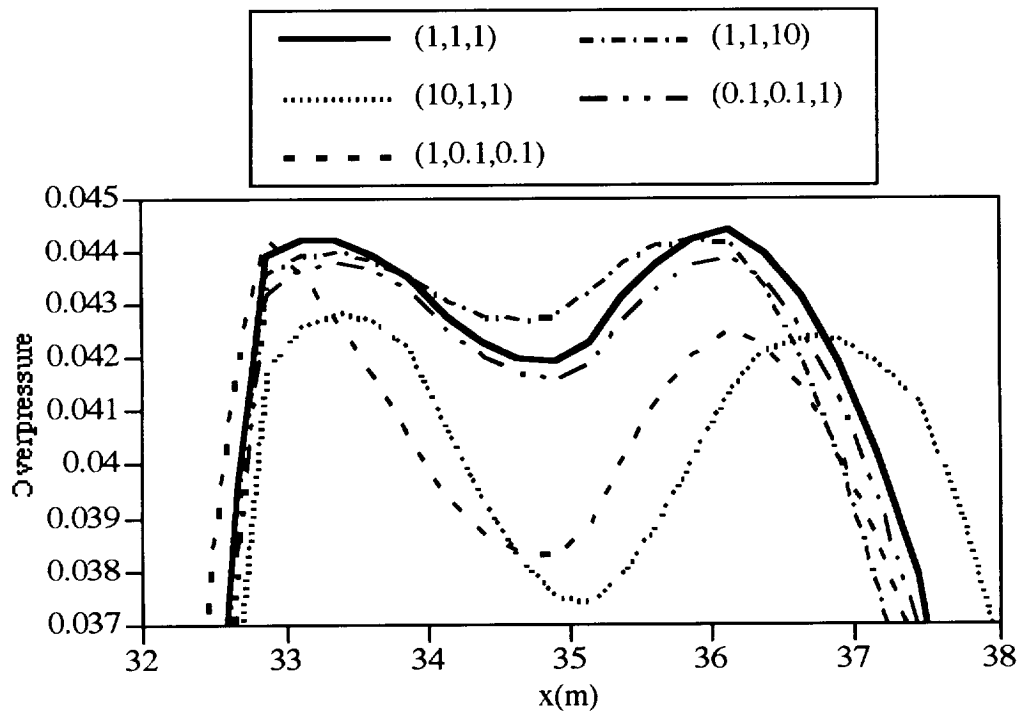
Table 3. Minimum  $C_D/C_L$  for weight factor sets.

	ref	(1,1,1)	(10,1,1)	(1,0.1,0.1)	(1,1,10)	(0.1,0.1,1)
$\lambda_1(\text{deg})$	70.46	72.86	74.50	72.84	72.32	72.51
$\lambda_2(\text{deg})$	52.42	51.43	52.87	50.50	50.81	50.58
$c_o(\text{m})$	7.81	8.29	8.67	8.30	7.96	7.86
$c_i(\text{m})$	1.5776	1.3510	1.2666	1.2632	1.3165	1.2400
$x_b(\text{m})$	11.99	12.51	13.00	12.39	12.36	12.30
$x_w(\text{m})$	7.80	7.56	7.71	7.27	7.62	7.66
$C_D/C_L$	0.11196	0.11049	0.11028	0.11016	0.11075	0.11077
		(-1.3%)	(-1.5%)	(-1.6%)	(-1.1%)	(-1.1%)
$(\Delta p_{\max})_2$	0.05206	0.04700	0.04336	0.04735	0.04680	0.04551
		(-9.7%)	(-17.2%)	(-9.0%)	(-10.1)	(-12.6)
cycle	-	29	28	27	18	27

Table 4. Minimum  $(\Delta p_{\max})_2$  for weight factor sets.

	ref	(1,1,1)	(10,1,1)	(1,0.1,0.1)	(1,1,10)	(0.1,0.1,1)
$\lambda_1(\text{deg})$	70.46	73.59	74.50	73.76	73.01	73.23
$\lambda_2(\text{deg})$	52.42	51.95	52.35	50.25	50.25	50.25
$c_o(\text{m})$	7.81	8.21	8.59	8.22	7.80	7.94
$c_i(\text{m})$	1.5776	1.3375	1.2794	1.2400	1.2400	1.2400
$x_b(\text{m})$	11.99	12.39	12.87	12.34	12.25	12.42
$x_w(\text{m})$	7.80	7.64	7.63	7.31	7.69	7.74
$C_D/C_L$	0.11196	0.11086	0.11035	0.11032	0.11100	0.11092
		(-1.0%)	(-1.4%)	(-1.5%)	(-0.9%)	(-0.9%)
$(\Delta p_{\max})_2$	0.05206	0.04442	0.04285	0.04428	0.04428	0.04391
		(-14.7%)	(-17.7%)	(-14.9%)	(-15.0)	(-15.7)
cycle	-	30	27	30	29	30

The corresponding pressure signatures for the minimum  $(\Delta p_{\max})_2$  cases are shown in Figures 16-17. As mentioned previously, all the weighted cases yielded a lower value of  $(\Delta p_{\max})_2$  than the unweighted case, with (10,1,1) yielding the lowest.

Figure 16. Pressure signatures for minimum  $(\Delta p_{\max})_2$  cases.Figure 17. The second pressure peak for minimum  $(\Delta p_{\max})_2$  cases.

One of the key issues to be addressed in the enhanced K-S function procedure is the proper choice of weight factors. In other words, the choice between Type A or Type B must be examined. Based on the results obtained in this study, Type B weight factors are recommended to be used with the developed procedure

## **REFERENCES**

1. McCarthy, T. and Chattopadhyay, A., "Multidisciplinary Optimization of Helicopter Rotor Blades Including Design Variable Sensitivity," *Proc. 4th AIAA/USAF/NASA/OAI Symposium on Multidisciplinary Analysis and Optimizations*, Cleveland, OH, September 1992. AIAA Paper No. 92-4750
2. Kreisselmeir, G. and Steinhauser, R. (1979) "Systematic Control Design by Optimizing a Vector Performance Index" *Proc. International Federation of Active Controls Symposium on Computer-Aided Design of Control Systems*, Zurich, Switzerland, Aug. 29-31, 1979, 113-117.
3. Wrenn, G. A., "An Indirect Method for Numerical Optimization Using the Kreisselmeier-Steinhauser Function," *NASA Contractor Report 4220*, 1989.
4. McCarthy, T., Chattopadhyay, A., and Zhang, S., "A Coupled Rotor/Wing Optimization Procedure of High Speed Tilt-Rotor Aircraft," presented at the *51st Annual Forum of the AHS*, May 9-11, 1995, Fort Worth, Texas.
5. Chattopadhyay, A., Narayan, J. R., Pagaldipti, N., Wensheng, X. and Cheung, S. H. "Optimization Procedure for Reduced Sonic Boom in High speed Flight." *AIAA Paper # 95-2156*, 26th AIAA Fluid Dynamics Conference, San Diego, California, June 1995.
7. Chattopadhyay, A., Jury IV, R. A. and Rajadas, J. N., "An Enhanced Multiobjective Formulation Technique For Multidisciplinary Design Optimization." *AIAA Paper 97 - 0104*. 35th Aerospace Sciences Meeting and Exhibit, Reno, Nevada, 1997.
6. Pagaldipti, N., Narayan, J. R. and Chattopadhyay, A., "Optimization Procedure With Analytical Aerodynamic Sensitivity for Reduced Sonic Boom Design," *AIAA Journal of Aircraft*, Vol. 33, No. 6, 1996, pp. 1123-1130.
8. Haftka, R. T., Gurdal, Z. and Kamat, M. P., "Elements of Structural Optimization," Kluwer Academic Publishers, Dordrecht, The Netherlands, 1990.
9. Chattopadhyay, A. and Pagaldipti, N., "A Multidisciplinary Optimization Using Semi-Analytical Sensitivity Analysis Procedure and Multilevel Decomposition," *Journal of Computers and Mathematics with Applications*, Vol. 29, No. 7, 1995, pp. 55-66.

10. Fadel, G. M., Riley, M. F. and Barthelemy, J. F. M., "Two-Point Exponential Approximation Method for Structural Optimization," *Structural Optimization*, 2, 1990, pp. 117-124.
11. Lawrence, S., Chaussee, D. and Tannehill, J., "Application of an Upwind Algorithm to the 3-D Parabolized Navier-Stokes Equations," AIAA Paper 87-1112, *AIAA 8<sup>th</sup> Computational Fluid Dynamics Conference*, Honolulu, Hawaii, June, 1987.
12. Rudman, S. and Rubin, S. G., "Hypersonic Viscous Flow Over Slender Bodies with Sharp Leading Edges," *AIAA Journal*, Vol. 6, 1968, pp. 1883-1889.
13. Lubard, S. C. and Helliwell, W. S., "Calculation of the Flow on a Cone at High Angle of Attack," *AIAA Journal*, Vol. 12, 1973, pp. 965-974.
14. Roe, P. L., "Approximate Riemann solver, Parameter Vectors and Difference Schemes," *Journal of Computational Physics*, Vol. 43, 1981, pp. 357-372.
15. Cheung, S. H., Edwards, T. A. and Lawrence, S. L., "Application of Computational Fluid Dynamics to Sonic Boom Near- and Mid-Field Prediction," *Journal of Aircraft*, Vol. 29, No. 5, 1992, pp. 920-926.
16. Whitham, G. B., "The Flow Pattern of a Supersonic Projectile," *Communications on Pure and Applied Mathematics*, Vol. 5, No. 3, 1952, pp. 301-348.
17. Hicks, R. and Mendoza, J., "Prediction of Aircraft Sonic Boom Characteristics from Experimental Near Field Results," NASA TMX1477, November 1967.



